J Electr Eng Technol Vol. 9, No. 5: 1527-1536, 2014
http://dx.doi.org/10.5370/JEET.2014.9.5.1527

ISSN(Print) 1975-0102
ISSN(Online) 2093-7423

Optimal Excitation Angles of a Switched Reluctance Generator for Maximum Output Power

Pairote Thongprasri† and Supat Kittiratsatcha*

Abstract – This paper investigates the optimal values of turn-on and turn-off angles, and ratio of flux linkage at turn-off angle and peak phase current positions of optimal control for accomplishing maximum output power in an 8/6 Switched Reluctance Generator (8/6 SRG). Phase current waveform is analyzed to determine optimal excitation angles (optimal turn-on and turn-off angles) of the SRG for maximum output power which is applied from a nonlinear magnetization curve in terms of control variables (dc bus voltage, shaft speed, and excitation angles). The optimal excitation angles in single pulse mode of operation are proposed via the analytical model. Simulated and experimental results have verified the accuracy of the analytical model.

Keywords: Switched reluctance generator, Output power, Excitation angles, Magnetization curve, Analytical model

1. Introduction

Switched reluctance generators (SRG) has been applied to many fields because of its merits such as low manufacturing cost, low inertia, fault tolerance [1, 2] high efficiency and reliability [3]. However, an SRG requires position sensor and produces acoustic noise and vibration [2, 3]. Torque production and energy conversion process of the SRG are described [4], and the SRG control systems for regulating speed and output power use a DSP controller as processor with excitation angles from a ROM-based table of switch positions. SRGs have proved for some applications, for example, starter/generator for gas turbine of aircrafts running at constant speed and connected to utility line [3] generating maximum output power depends on optimal excitation angles due to dc bus voltage and shaft speed are constant, wind generator connected with a fixed voltage unity line [5] so maximum output power depends on optimal excitation angles at each shaft speed, starter alternator in car [6] generating maximum output power depends on optimal excitation angles at each shaft speed and dc bus voltage due to its voltage may change during charging or discharging periods. To control generating maximum output power of SRG we must know relationship of control variables included dc bus voltage, shaft speed, and excitation angles. However there is no analytical equation for output power in terms of design parameters and control variables due to highly nonlinear characteristics of an SRG, therefore iterative simulation and experiments of an SRG have been used for finding output power profile [7]. Almost simulation models used to study generating maximum output power of SRG are based on lookup-table techniques [8], magnetic equivalent circuit analysis [9], cubic-spline interpolations [10], and finite-element analysis (FEA) [11] which are very accurate, however these models require either numerous values of flux-linkage and current position or information magnetic properties about an SRG. A simple model of the nonlinear magnetization characteristics of an SRG has been proposed [12, 13] which is easy to build, its accuracy, and the machine geometry is unknowable. Finding the output power requires the knowledge of the current waveform that the expression of phase current based on magnetic field energy proposed [14] for applying to optimize method of firing based on simulations is reliable but complicated. The closed loop power control algorithm for the SRG which relies on experimental characterization at only four operating points, turn-on and turn-off angles, speed, and power, is presented [16]. Analysis of the phase inductance and the phase current divided into five periods during the excitation period and commutation period of an SRG for creating the triggering signals of the main switches are described [17]. The relationship between commutation angles and output power is described [18] that the impact of changes in excitation angles on the output voltage or power had been examined by applying various combinations of turn-on and turn-off angles. Phase current and phase flux linkage of an SRG with optimal excitation angles obtained from a nonlinear SRG model based on MATLAB/SIMULINK are analyzed to find the relationship between the conventional and freewheeling excitation patterns through SF-transform for output power maximization and optimal symmetric freewheeling excitation [19].

From those described above, there is no analytical equation for output power in terms of control variables due

† Corresponding Author: Faculty of Engineering, King Mongkut's Institute of Technology Ladkrabang, Thailand. (sfengprt@src.ku.ac.th)
* Faculty of Engineering, King Mongkut's Institute of Technology Ladkrabang, Thailand. (kksupat@kmitl.ac.th)
Received: May 22, 2013; Accepted: September 16, 2013

to highly nonlinear characteristics of an SRG, and phase current is significant parameter to find optimal excitation angles of an SRG for maximum output power. In this paper the mathematical expression of a nonlinear magnetization curve used is simple that depends on the two magnetization curves in aligned and unaligned positions of the rotor, phase current waveform used to determine optimal excitation angles of an 8/6 SRG is applied from a nonlinear magnetization curve in term of control variables included dc bus voltage (u), shaft speed (ω), and excitation angles ((turn-on (θ_{on}) and turn-off (θ_{off}) angles) and its effectiveness is validated through simulated and experimental results.

2. Analysis of SRG Operation

SRG is a machine which excitation energy is supplied in every stroke. During the conducting period $\theta_{on} - \theta_{off}$ (Fig. 1), the excitation energy is converted to electrical energy after the aligned angle. No energy is supplied to the load during the conducting period. During the de-fluxing period $\theta_{off} - \theta_{ext}$ (Fig. 1), the store field energy is released as output energy through the freewheeling diodes (Fig. 2). The electrical energy produced during the de-fluxing period exceeds the excitation energy. The phase voltage has just θ_{on} and θ_{off} switching angles as shown in Fig. 1.

Figs. 1(a) - (c) show idealized current waveforms with single pulse control that the peak current occurs at $\theta_{off} - \theta_{peak}$. Fig. 1(a) shows the case that the current increase after turning off the switches at θ_{off}, when the back emf in the coil is larger than the dc bus voltage $(e > u)$. Fig 1(b) shows the case that the constant current after turning off the switches at θ_{off} until θ_{peak}, when the back emf and the dc bus voltage balance $(e = u)$. Fig. 1(c) shows the case that the current decrease after turning off the switches at θ_{off}, when the back emf in the coil is smaller than the dc bus voltage $(e < u)$. The control method which regulates u with speed in order to maximize the output power by keeping the condition of $u = e$ is proposed [1, 15].

In this paper, the control scheme of an 8/6 SRG for maximum output power which controls the current

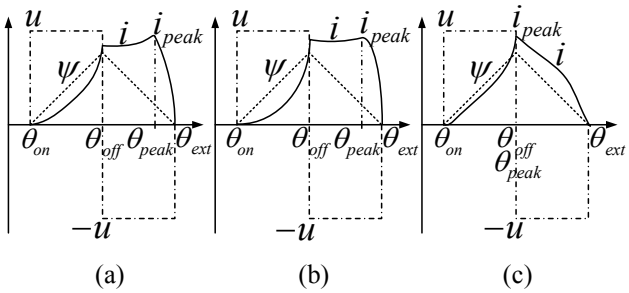

Fig. 1. Phase of voltage and current, and flux linkage

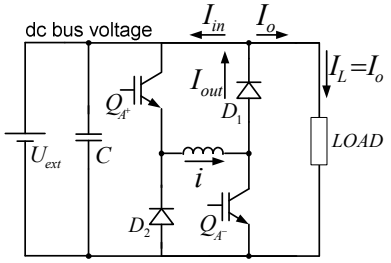

Fig. 2. Generator circuit for a phase

waveform like the case of $e = u$ is proposed. The analytical model and its accuracy are validated through simulated and experimental results.

The voltage equation for a phase of the switched reluctance machine by neglecting the mutual inductance between the phases is given as:

$$u = Ri + L\frac{di}{dt} + e \tag{1}$$

Where u is the dc bus voltage, i is the phase current, R is the phase resistance, L is the phase inductance, e is the back emf, θ is the rotor position, and ω is the shaft speed. The back emf is defined as $e = \omega i \frac{dL}{d\theta}$.

Phase resistance variation is small and ohmic drop on phase resistance is usually negligible compared to dc bus voltage, so we don't consider phase resistance variation in our analysis, flux linkage equals to:

$$\Psi = \int_0^t u dt = \frac{u}{\omega}\begin{cases}(\theta - \theta_{on}), & \theta_{on} < \theta \le \theta_{off} \\ (\theta_{ext} - \theta), & \theta_{off} < \theta \le \theta_{ext} \\ 0\ , & else\end{cases} \tag{2}$$

Where extinct angle $(\theta_{ext}) = 2\theta_{off} - \theta_{on}$. The circuit diagram of a generator with one phase leg has been proposed [1] as shown in Fig. 2. The integral of the currents in Fig. 2 can be defined as:

$$I_{in} = \frac{1}{2\pi}\int_{\theta_{on}}^{\theta_{off}} i d\theta \tag{3}$$

$$I_{out} = \frac{1}{2\pi}\int_{\theta_{off}}^{\theta_{ext}} i d\theta \tag{4}$$

The net generated current $(I_o) = I_{out} - I_{in}$, and phase output power $(P_{out}) = u \cdot I_o$.

3. Phase Current Formulation

In earlier contribution of magnetization curve in Fig. 3 proposed [12, 13]; at unaligned position (θ_u) is linear to phase current, and at aligned position (θ_a) approximated by two curves composes of a straight line from coordinate origin O to point S and a curve from point S to point M. An analytical model proposed [12, 13] can describe

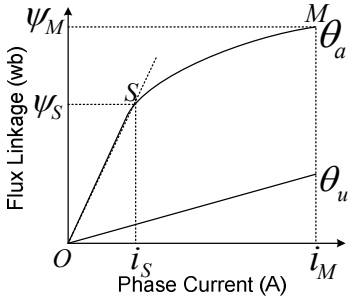

Fig. 3. Flux linkage curves in θ_u and θ_a

magnetization characteristics of machines with sufficient accuracy. This analytical model described by flux linkage depends on phase current and rotor position as shown in (5).

$$\Psi(i,\theta) = \frac{1}{2}[\Psi_a(i) - \Psi_u(i)]\left[cos\left(N_r\left(\theta + \frac{2\pi}{N_r}\right)\right) + 1\right] + \Psi_u(i) \quad (5)$$

When

$$\Psi_u(i) = L_u \cdot i$$

$$\Psi_a(i) = \begin{cases} L_a \cdot i\ , & i \le i_S \\ \Psi_{S0} + \sqrt{4a(i - i_{S0})}, & i > i_S \end{cases}$$

$$i_{S0} = i_S - \frac{a}{L_a^2}, \Psi_{S0} = \Psi_S - \frac{2a}{L_a}$$

$$\Psi_{MS} = \Psi_M - \Psi_S,\ \ i_{MS} = i_M - i_S$$

$$a = \frac{\Psi_{MS}^2}{4(i_{MS} - \frac{\Psi_{MS}}{L_a})}$$

Where L_u is inductance of the coil for the unaligned position, L_a is inductance of the coil for the aligned position, N_r is pole number of rotor, θ is rotor angle in radian. Note that Ψ_S, i_S and Ψ_M, i_M are the values of the flux and current taken at points *S* and *M* respectively.

Table 1 shows parameters of the candidate SRG used in this paper which has eight poles on the stator and six poles

Table 1. Parameters of the candidate SRG

Parameter	Value
Outer diameter of stator	150 mm
Inner diameter of stator	70 mm
Length of air gap	0.5 mm
Stator pole arc	22°
Rotor pole arc	24°
Stack length	70 mm
Numbers of phases	4 Phase
Numbers of poles	8/6
Rated Power	2.23kW
Rated Voltage	48V
Aligned Inductance	490μH
Unaligned Inductance	40μH

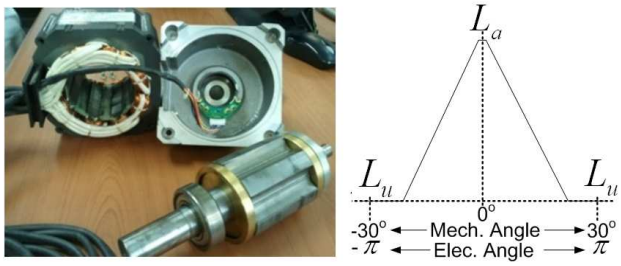

(a) (b)

Fig. 4. The candidate SRG used in paper: (a) Structure of the 8/6 SRG; (b) Idealized inductance versus rotor position

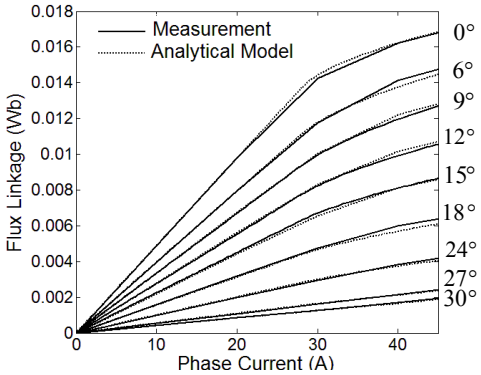

Fig. 5. Magnetization curves of the candidate SRG

on the rotor as shown in Figs. 4(a), and (b) shows idealized inductance versus rotor position.

Fig. 5 shows the magnetization curves of the candidate SRG at different rotor positions, both from measurement and the analytical model proposed [12, 13]. Parameters of the analytical model used to calculate in (5) are $L_u = 40\mu H$, $L_a = 490\mu H, i_S = 25A, i_M = 45A, \Psi_S = 0.0125Wb$, and $\Psi_M = 0.017Wb$.

The significant variable to control an SRG for maximum output power is phase current. The phase current equation in this paper obtains from substituting (2) into (5). Since the magnetization curve in Fig. 3 approximated by two curves composes of a straight line from coordinate origin O to point S therefore phase current in this period ($i \le i_S$) can be obtained from (6) and a curve from point S to point M therefore phase current in this period ($i > i_S$) can be obtained from (7).

$$i = \frac{2c}{L_a(k+1) + L_u(1-k)}, \quad i \le i_S \quad (6)$$

$$A \cdot i^2 + B \cdot i + C = 0, \ \ i > i_S \quad (7)$$

Where

$$c = \frac{u}{\omega}\begin{cases} (\theta - \theta_{on}), & \theta_{on} < \theta \le \theta_{off} \\ (\theta_{ext} - \theta), & \theta_{off} < \theta \le \theta_{ext} \\ 0\ , & else \end{cases}$$

$$k = cos\left[N_r\left(\theta + \frac{2\pi}{N_r}\right)\right]$$
$$A = \left[\frac{L_u^2(k-1)^2}{4a(k+1)^2}\right]$$
$$B = \left[\frac{4L_u \cdot c(k-1) + 2\Psi_{S0} \cdot L_u(1-k^2)}{4a(k+1)^2} - 1\right]$$
$$C = \left[\frac{\Psi_{S0}^2(k+1)^2 - 4\Psi_{S0} \cdot c(k+1) + 4c^2}{4a(k+1)^2} + i_{S0}\right]$$

4. Optimal Excitation Angles

The case of $P_{out} = f(\theta_{on}, \theta_{off})$ when dc bus voltage (u) and shaft speed (ω) are constant, therefore output power will be a constant function of just switching angles proposed [7]. In Fig. 6 shows the relationship of phase current and flux linkage waveforms, when conducting period is equals to de-fluxing period. Flux linkage at θ_{off} and θ_{peak} positions are defined as Ψ_f and Ψ_k respectively, and their equations are given as:

$$\Psi_f = \int_{\theta_{on}}^{\theta_{off}} \frac{u}{\omega} d\theta = \frac{u}{\omega}(\theta_{off} - \theta_{on}) \quad (8)$$

$$\Psi_k = \int_{\theta_{peak}}^{\theta_{ext}} \frac{u}{\omega} d\theta = \frac{u}{\omega}(\theta_{ext} - \theta_{peak}) \quad (9)$$

To simplify the analysis, $x$is defined as a ratio ofΨ_k and Ψ_f that it can be expressed as:

$$x = \frac{\theta_{ext} - \theta_{peak}}{\theta_{off} - \theta_{on}} = \frac{2\theta_{off} - \theta_{on} - \theta_{peak}}{\theta_{off} - \theta_{on}} \quad (10)$$

Then (10) can be rewritten as:

$$\theta_{off} = \frac{(x-1)\cdot\theta_{on} - \theta_{peak}}{(x-2)} \quad (11)$$

Phase current depends on dc bus voltage, shaft speed, and excitation angles that peak phase current (i_{peak}) at θ_{peak} position can occur in during generation period.

$$\left.\frac{di}{d\theta}\right|_{\theta_{peak}} = 0, \ \theta_{off} < \theta \leq \theta_{ext}$$

Then θ_{peak} can be obtainedas follow:

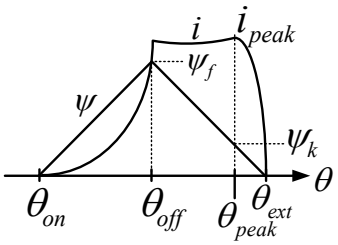

Fig. 6. Idealized of phase current and flux linkage.

$$sin\left[N_r\left(\theta_{peak} + \frac{2\pi}{N_r}\right)\right] = \begin{cases} \frac{i_{peak}}{2N_r\left(\frac{u}{\omega}\right)(L_a - L_u)} & , i \leq i_s \\ \frac{N_r\sqrt{4a(i_{peak} - i_{s0}) - L_u \cdot i_{s0} + \Psi_{s0}}}{2\left(\frac{u}{\omega}\right)} & , i > i_S \end{cases} \quad (12)$$

An SRG operates in single pulse mode, the phase current waveforms of the SRG limited the peak value to be equal can occur in three cases as shown in Fig. 1, and when the SRG is controlled with the constant of dc bus voltage and shaft speed therefore the peak phase current can be known by; to simplify the analysis, y is defined as a ratio of the dc bus voltage and the shaft speed and y_{opt} is defined as a ratio of the dc bus voltage and the shaft speed at peak phase current, in (12) implies that the peak phase current can exist either at turn-off position or after, the value of $sin\left[N_r\left(\theta_{peak} + \frac{2\pi}{N_r}\right)\right]$ in (12) never exceeds 1. Those mean a ratio of the dc bus voltage and the shaft speed at peak phase current$\left(\left.\frac{u}{\omega}\right|_{i_{peak}} = y_{opt}\right)$ can be expressed as:

$$y_{opt} = \begin{cases} \frac{i_{peak}}{2N_r(L_a - L_u)} & , i \leq i_S \\ \frac{N_r\sqrt{4a(i_{peak} - i_{s0}) - L_u \cdot i_{s0} + \Psi_{s0}}}{2} & , i > i_S \end{cases} \quad (13)$$

To find the optimal turn-on angle $(\theta_{on.opt})$ the analytical model is simulated for three cases of y; $y = 0.042$, $y = 0.044$, and $y = 0.046$ that all cases are fixed u at 27V when the excitation angles were adjusted to limit the peak value of the phase current to 45A, and the output power (4-phase) can be known by $P_{out} = 4 \times (u \cdot I_o)$. There are many combinations of turn-on and turn-off angles as shown in Fig. 7. Apparently the maximum output power exists at turn-on angle at -15° for all cases as shown in Fig. 7(a). This simulation result has been also confirmed [7]. Also in this paper the value of optimal turn-on angle $(\theta_{on,opt})$ is -15°. Fig. 7(b) shows output power versus turn-off angle.

Fig. 8(a) shows the phase current waveforms with single

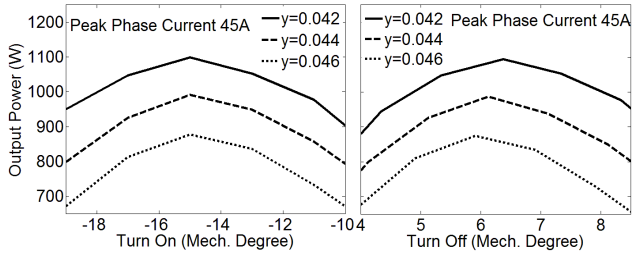

(a) (b)

Fig. 7. Output power at different excitation angles: (a) Output power versus turn-on angle (b) Output power versus turn-off angle.

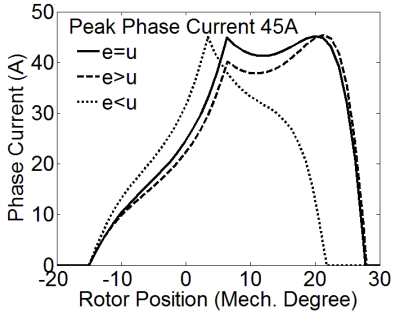

(a) Phase current waveforms

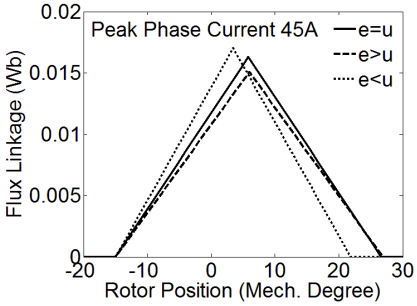

(b) Flux linkage waveforms

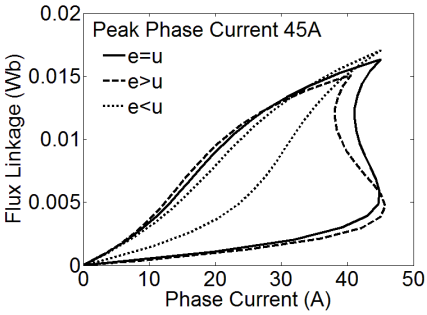

(c) Energy conversion loops

Fig. 8. Phase current and flux linkage waveforms, and energy conversion loops in single pulse mode of operation

pulse control at $y = 0.038$, $y = 0.042$, and $y = 0.048$ with u = 27V for all cases when excitation angles were adjusted to limit the peak value of the phase current to 45A, Fig. 8(b) shows their flux linkage waveforms for three cases based on (5) with $L_u = 40\mu H$, $L_a = 490\mu H$, $i_S = 25A$, $i_M = 45A$, $\Psi_S = 0.0125Wb$, and $\Psi_M = 0.017Wb$, and Fig. 8(c) shows their energy conversion loops. For peak phase current at 45A, consequently the y_{opt} based on (13) is 0.042. Simulation results; the case of $y = 0.048$ or $y > y_{opt}$ back emf in the coil is smaller than dc bus voltage $(e < u)$ and the current decreases after θ_{off}, the case of $y = 0.042$ or $y = y_{opt}$ back emf in the coil and dc bus voltage balance $(e = u)$ and the current stays constant from θ_{off} until θ_{peak} that the SRG generates maximum output power confirmed [1, 15], and the case of $y = 0.038$ or $y < y_{opt}$ back emf in the coil is larger than dc bus voltage $(e > u)$ and the current increases after θ_{off}.

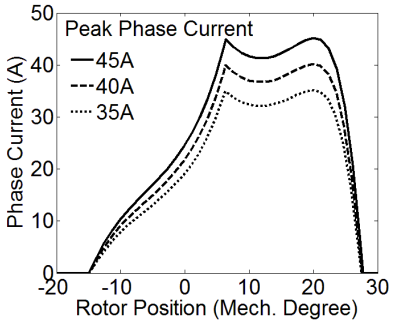

Fig. 9. Phase current waveforms with optimal excitation angles

To find the optimal value of $x(x_{opt})$ that the θ_{peak} needs to be resolved using the relation of θ_{peak} with i_{peak} based on (12). Phase current in case of $e = u$ in Fig. 8(a), the x_{opt} can be known by calculating in (10) that is 0.266.

The optimal turn-off angle $(\theta_{off.opt})$can be known by substituting x_{opt} and θ_{peak} into (11).

To validate the value of x_{opt}, Fig. 9 shows three phase current waveforms based on (6) and (7) that limit the peak value of the phase current to 35A, 40A, and 45A. The values of $\theta_{on,opt}$, x_{opt}, and u for three cases are fixed at -15°, 0.266 and 27V respectively. θ_{peak} and $\theta_{off.opt}$ can be known by calculating in (12) and (11) respectively. Simulation results, waveforms of the phase current for all three cases are similar to phase current waveform in case of $e = u$.

5. Experimental Results

The proposed model is verified via comparison with laboratory measurements, the schematic layout of the experimental system is shown in Fig. 10(a), and the test-bed in laboratory is established shown in Fig. 10(b). The 3-phase induction motor drives the 8/6 SRG which is excited through a 4-phase asymmetrical converter. This converter uses the same dc source for excitation through the IGBTs and demagnetization through the diodes. The converted energy supplies to a sufficiently stiff dc source to prevent the dc bus level running away during generation period. The rotary encoder provides rotor position as pulse train (3,600count/rev) to TMS320F2812 DSP controller. The values of excitation angles which drive the gate of converter are processed by the controller. The y ratio can be controlled by adjusting dc bus voltage and shaft speed. The output power has been measured on a test-bed of variations of ratio of dc bus voltage and shaft speed, and excitation angles.

For experiment to validate the value of x_{opt}; Fig. 11(a) shows the measured waveforms of phase of voltage and current and average output of voltage and current when the SRG is controlled to limit i_{peak} to 45A with the optimal excitation angles. The u and ω used for experiment are

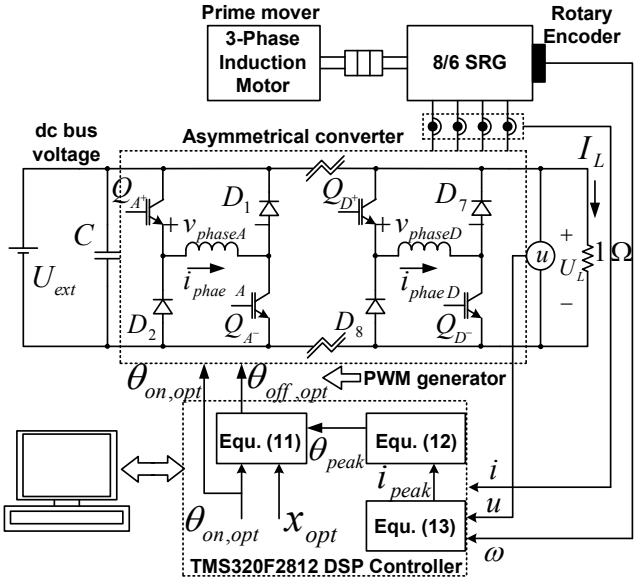

(a) Schematic layout of the experimental system

(b) Converter and a TMS320F2812 DSP Controller, Prime mover and the SRG, and Resistive load

Fig. 10. Experimental setup, converter, load and SRG

27V and 642 rad/s respectively that the values of $\theta_{on,opt}$ and x_{opt} obtained from the simulation results of analytical model are -15° and 0.266 respectively. For $\theta_{off.opt}$ is 6.34° based on (11), Fig. 12(a) shows the measured waveforms of phase of voltage and current and average output of voltage and current when the SRG is controlled to limit i_{peak} to 45A with u and ω used for experiment are 27V and 717 rad/s respectively that the values of θ_{on} and x are -15° and 0.253 respectively. For θ_{off} is 6.75° based on (11), Fig. 13(a) shows the measured waveforms of phase of voltage and current and average output of voltage and current when the SRG is controlled to limit i_{peak} to 45A with u and ω used for experiment are 27V and 558 rad/s respectively that the values of θ_{on} and x are -15° and 1 respectively. For θ_{off} is 4.40° based on (11), and Figs. 11(b), 12(b), and 13(b) show phase current waveform both from measurement and analytical model.

Experimental results; the SRG controlled with optimal excitation angles in Fig. 11 generates maximum output power that the optimal excitation angles are θ_{on} = -15° and θ_{off}= 6.34°.

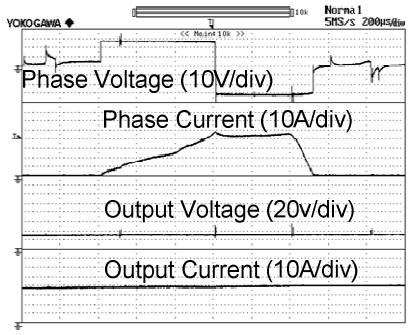

(a) $x = x_{opt}$; x = 0.266

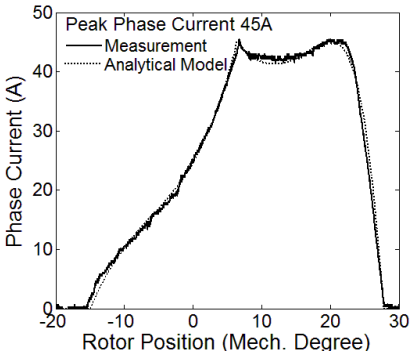

(b) θ_{on}= -15°θ_{off}= 6.34°

Fig. 11. Optimal excitation angle for $x = x_{opt}$ (I_L = 39.86A, U_L = 27.6V, P_{out} = 1100.14W)

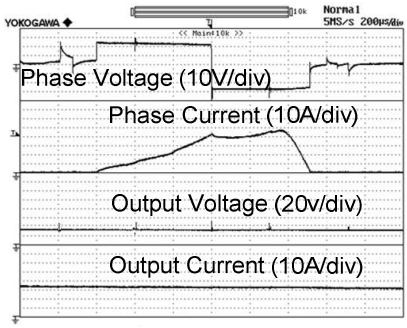

(a) $x < x_{opt}$; x = 0.253

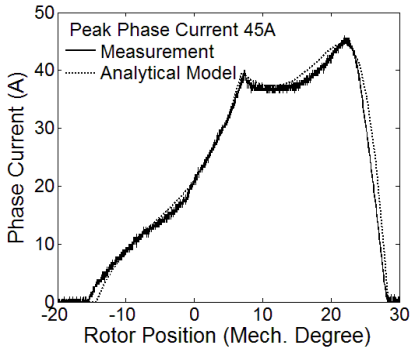

(b) θ_{on}= -15°θ_{off}= 6.75°

Fig. 12. Excitation angle for $x < x_{opt}$ (I_L = 31.97A, U_L = 27.52V, P_{out} = 879.81W)

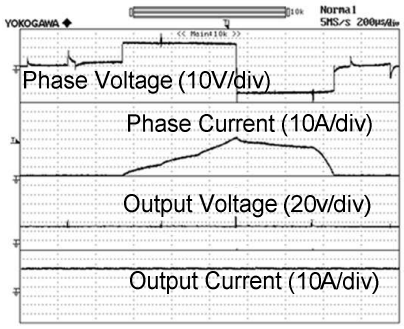

(a) $x > x_{opt}$; $x = 1$

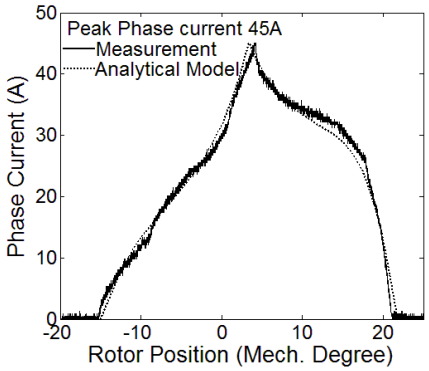

(b) θ_{on}= -15°θ_{off}= 4.40°

Fig. 13. Excitation angle for $x > x_{opt}$ ($I_L = 20.6\text{A}$, $U_L = 27.68\text{V}$, $P_{out} = 570.21\text{W}$)

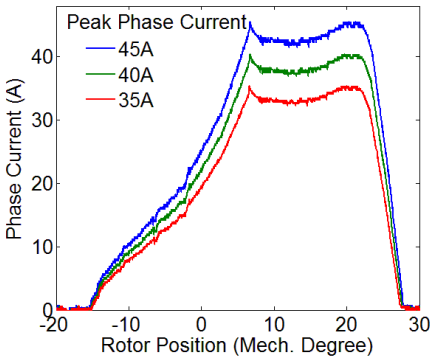

Fig. 14. Phase current waveforms with x_{opt} = 0.266 for all three cases of i_{peak}; 35A, 40A, and 45A

Table 2. Parameters for three cases of phase current

u (V)	ω (rad/s)	i_{peak} (A)	θ_{on} (°)	θ_{off} (°)	θ_{peak} (°)	θ_{ext} (°)	x
27	757	35	-15	6.26	21.86	27.52	0.266
27	692	40	-15	6.30	21.93	27.60	0.266
27	642	45	-15	6.34	22	27.68	0.266

For experiment to validate the value of x_{opt}, Fig. 14 shows the measured phase current waveforms for all three cases of i_{peak}; 35A, 40A, and 45A. Table 2 shows the optimal control variables for all three cases that the values

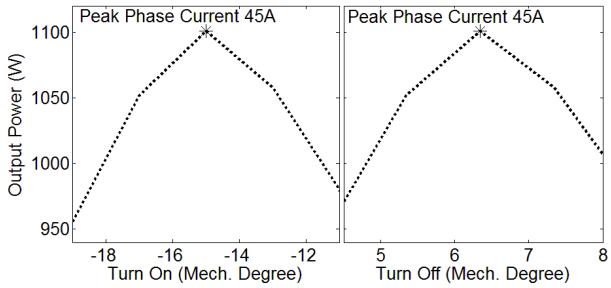

(a) P_{out}vsθ_{on} (b) P_{out} vs θ_{off}

Fig. 15. Output power at different excitation angles; case 1

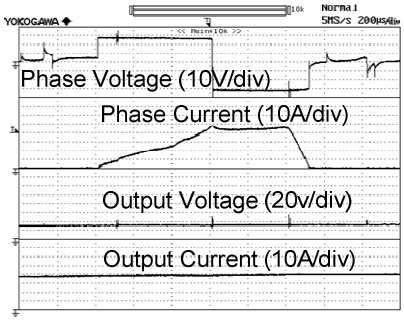

Fig. 16. Optimal excitation angles (θ_{on}=-15°θ_{off}=6.34°) ($I_L = 39.86\text{A}$, $U_L = 27.6\text{V}$, $P_{out} = 1100.14\text{W}$)

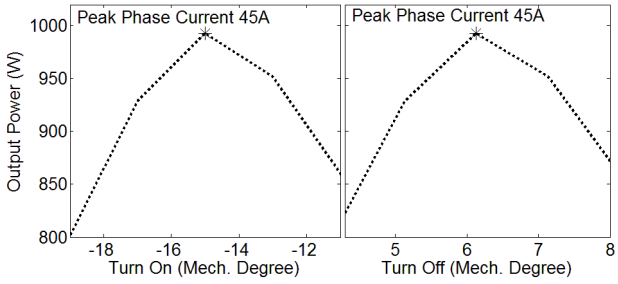

(a)P_{out}vsθ_{on}(b) P_{out} vsθ_{off}

Fig. 17. Output power at different excitation angles; case 2

Table 3. Parameters for three cases

Case	u (V)	ω (rad/s)	i_{peak} (A)	$\theta_{on,opt}$ (°)	x_{opt}	$\theta_{off,opt}$ (°)
1	27	642	45	-15	0.266	6.34
2	27	656	45	-15	0.266	6.13
3	27	740	45	-15	0.266	5.91

of $\theta_{on,opt}$, x_{opt}, and u for three cases are fixed at -15°, 0.266 and 27V respectively and $\theta_{off.opt}$ can be known by calculating in (11). Experimental results, waveforms of the phase current for all three cases are similar to phase current waveform in case of $e = u$.

For experiment to validate the optimal excitation angles for three cases when u is fixed; Figs. 15, 17, and 19 show output power versus different excitation angles when excitation angles were adjusted to limit $i_{peak} = 45\text{A}$ for

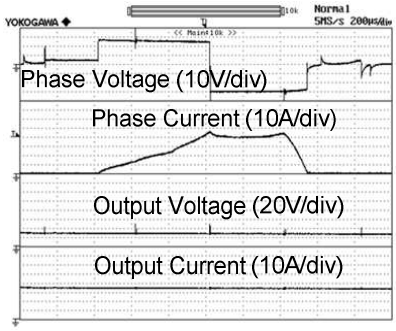

Fig. 18. Optimal excitation angles (θ_{on}=-15°θ_{off}=6.13°) ($I_L = 35.97$A, $U_L = 27.6$V, $P_{out} = 992.77$W)

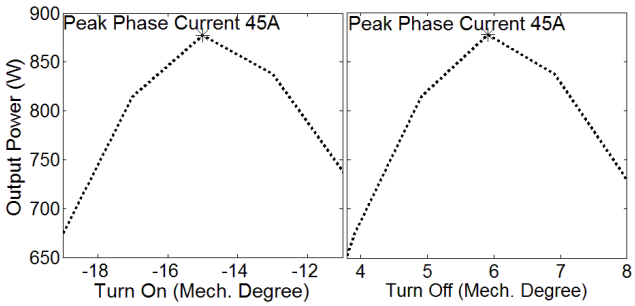

(a) P_{out}vsθ_{on} (b) P_{out} vs θ_{off}

Fig. 19. Output power at different excitation angles; case 3

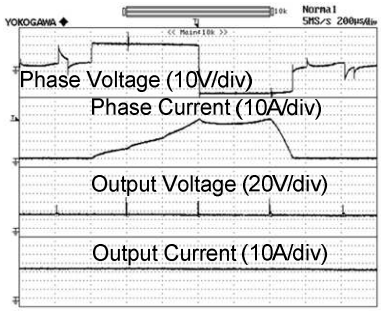

Fig. 20. Optimal excitation angles (θ_{on}=-15°, θ_{off}=5.91°) ($I_L = 31.78$A, $U_L = 27.6$V, $P_{out} = 877.13$W)

Table 4. Optimal control variables

u (V)	ω (rad/s)	i_{peak} (A)	$\theta_{on,opt}$ (°)	θ_{peak} (°)	θ_{ext} (°)	x_{opt}	$\theta_{off,opt}$ (°)
21	656	30	-15	21.81	27.46	0.266	6.23
27	642	45	-15	22	27.68	0.266	6.34
37	740	60	-15	22.28	28	0.266	6.50

all three cases with the values of u and ω shown in Table 3. The values of optimal excitation angles based on the proposed method are shown in Table 3 that the SRG generates maximum output power and the waveforms of phase current for case 1 to case 3 are shown in Figs. 16, 18, and 20 respectively.

For experiment to validate the optimal excitation angles

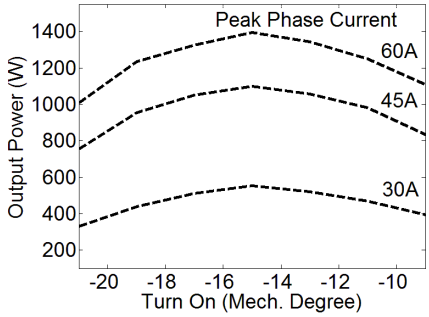

(a) P_{out}vs θ_{on}

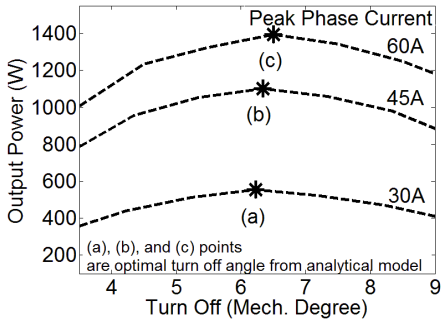

(b) P_{out}vs θ_{off}

Fig. 21. Output power at different excitation angles

with different u and ω, all dashed lines obtained from measurements in Fig. 21 show output power versus different excitation angles when excitation angles were adjusted to limit peak phase current for three cases; 30A, 45A, and 60A, with u and ω as shown in Table 4. Experimental results; maximum output power apparently exists at turn-on angle at -15° for all cases as shown in Fig. 21(a), three points; (a), (b), and (c), of noted by asterisk in Fig. 21(b) are the $\theta_{off.opt}$ based on (11) as shown in table 4 and Figs. 22(a)-(c) show phase of voltage and current, and average output of voltage and current when the SRG controlled with the optimal excitation angles generates maximum output power.

6. Conclusion

Optimal excitation angles of an 8/6 SRG analyzed from phase current waveform are presented in this paper. The phase current equation is significant factor for determining the optimal excitation angles that depends on optimal values of excitation angles ($\theta_{on,opt}$ and $\theta_{off,opt}$), a ratio of flux linkage at turn-off angle and peak phase current positions (x_{opt}). The analytical model is applied from a nonlinear magnetization curve in terms of dc bus voltage (u), shaft speed (ω), and excitation angles (θ_{on} and θ_{off}). The experimental results have confirmed the accuracy of the analytical model for determining the optimal excitation angles of the SRG for maximum output power. All cases for the SRG controlled with the optimal excitation angles

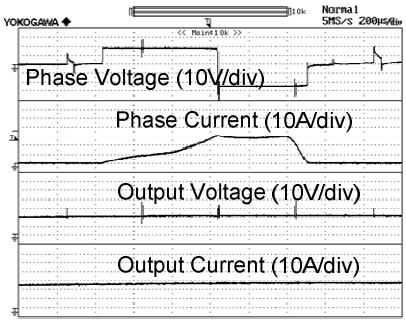

(a) Optimal excitation angles (θ_{on}= -15°, θ_{off}= 6.23°) ($I_L = 25.87$A, $U_L = 21.4$V, $P_{out} = 553.62$W)

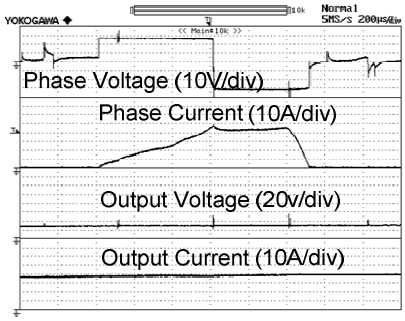

(b) Optimal excitation angles (θ_{on}= -15°, θ_{off}= 6.34°) ($I_L = 39.86$A, $U_L = 27.6$V, $P_{out} = 1100.14$W)

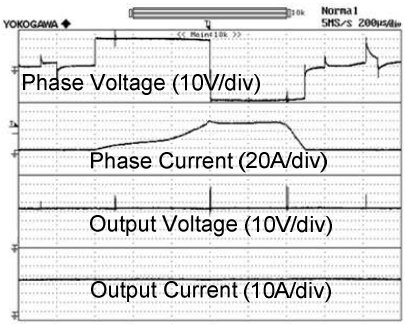

(c) Optimal excitation angles (θ_{on}= -15°, θ_{off}=6.50°) ($I_L = 37.27$A, $U_L = 37.4$V, $P_{out} = 1393.9$W)

Fig. 22. Optimal excitation angles at (a) $i_{peak} = 30$A, $(b) i_{peak} = 45$A, and $(c) i_{peak} = 60$A

in single pulse mode of operation generate maximum output power and phase current waveforms are similar to the case of $e = u$. Simulation and experimental results; the value of $\theta_{on,opt}$ is -15°, the value of $\theta_{off,opt}$ can be known by substituting x_{opt} = 0.266 and θ_{peak} into (11).

References

[1] T. J. E. Miller, "Electronic Control of Switched Reluctance Machines", Oxford, *UK*,*Newnes*, 2001.

[2] K. Xin, Q. Zhan, and J. Luo, "A New Simple Sensor less Control Method for Switched Reluctance Motor Drives", *Journal of ElecEng& Tech*, Vol.1, no. 1, pp. 52-57, 2006.

[3] C. A. Ferreira, S. R. Jones, W. S. Heglund, and W. D. Jones, "Detailed Design of a 30-kW Switched Reluctance Starter/Generators System for a Gas Turbine Engine Application*", IEEE Trans on IndAppl*, vol. 31, no. 3, pp.553-561, 1995.

[4] D. A. Torrey, "Switched Reluctance Generators and Their Control", *IEEE Trans on IndElec*, vol. 49, no. 1, pp. 3-14, 2002.

[5] R. Cardenas, W. F. Ray, and G. M. Asher, "Swithced Reluctance Generators for Wind Energy Applications", *Proc IEEE*, pp. 559-564, 1995.

[6] B. Fahimi, A. Emadi, and R. B. SepeJr, "A switched Reluctance Machine-Base Startor/Alternator for More Electic Cars", *IEEE Trans on EnergConv*, vol. 19, no. 1, pp. 116-124, 2004.

[7] P. Asadi, M. Ehsani, and B. Fahimi. "Design and Control Characterization of Switched Reluctance Generator for Maximum Output Power", *Proc IEEE*, pp. 1639-1644, 2006.

[8] F. Soares and P. J. C. Branco, "Simulation of a 6/4 Switched Reluctance Motor Based on Matlab/ Simulink Environment", *IEEE Trans on Aero and Elec Sys*, vol. 37, no. 3, pp. 989-1009, 2001.

[9] J. M. Kokernak and D. A. Torrey, "Magnetic Circuit Model for the Mutually Coupled Switched-Reluctance Machine", *IEEE Trans on Mag*, vol. 36, no. 2, pp. 500-507, 2000.

[10] D. W. J. Pulle, "New Data Base for Switched Reluctance Drive Simulation", *Proc. IEE on ElecPowAppl*, vol. 138, no. 6, pp. 331-337, 1991.

[11] Y. Xu and D. A. Torrey, "Study of the Mutually Coupled Switched Reluctance Machine Using the Finite Element-Circuit Coupled Method", *Proc. IEE on ElecPowAppl*, vol. 149, no. 2, pp. 81-86, 2002.

[12] C. Roux and M. M. Morcos, "On the Use of a Simplified Model for Switched Reluctance Motors", *IEEE Trans on EnerConv*, vol. 17, no. 3, pp. 400- 405, 2002.

[13] Y. Cai, Q. Yang, L. Su, Y. Wen, and Y. You, "Nonlinear Modeling for Switched Reluctance Motor by Measuring Flux Linkage Curves", *ProcIEEE on Com Eng and Tech*, V6-47-V6-51, 2010.

[14] X. Cao, Z. Deng, T. Yao, J. Cai, and Z. Zhuang, "Analysis and Application of Phase Current in Switched Reluctance Generators", *IEEE Trans. on Appl Sup*, vol. 20, no. 3, pp. 1063-1067, 2010.

[15] T. Sawata. P. C. Kjaer, C. Cossar, and T. J. E. Miller, "A Control Strategy for the Switched Reluctance Generator", *ProcICEM on Elec Mach and Sys*, pp. 2131-2136, 1998.

[16] Y. Sozer and D. A. Torrey, "Closed Loop Control of Excitation Parameters for High Speed Switched-Reluctance Generators", *IEEE Trans on PowElec*, vol. 19, no. 2, pp. 355-362, 2004.

[17] H. Chen and J. J. Gu, "Implementation of the Three-Phase Switched Reluctance Machine System for Motors and Generators", *IEEE/ASME Trans on Mech*, vol. 15, no. 3, pp. 421-432, 2010.
[18] M. Ziapour, E. A fjei, and M. Yousefi. "Optimam Commutation Angles for Voltage Regulation of a High Speed Switched Reluctance Generator", *Proc PEDST,* pp. 271-276, 2013.
[19] V. Nasirian, S. Kaboli and A. Davoudi, "Output power Maximization and Optimal Symmetric Freewheeling Excitation for Switched Reluctance Generators", *IEEE Trans on IndAppl*, vol. 49, no. 3, pp. 1031-1042, 2013.

Pairote Thongprasri He received M. Eng. Degree in electrical engineering from KMITL. Now he is studying in D. Eng. Program (electrical engineering) at KMITL. His research interests are switched reluctance machine and power electronics.

Supat Kittiratsatcha He received the M.S. and Ph.D. degrees in electric power engineering from Rensselaer Polytechnic Institute, Troy, NY. He is an Associate Professor with the Department of Electrical Engineering at KMITL. His research interests include switched reluctance machine design and solid state lighting.